Phonon calculations of thermodynamic properties of solid ^{4}He above its high-pressure triple point

P. Loubeyre
Physique des Milieux très Condensés, Université Pierre et Marie Curie, 75230 Paris Cédex 05, France

D. Levesque and J. J. Weis
Laboratoire de Physique Théorique et Hautes Energies, Université de Paris—Sud, 91405 Orsay, France
(Received 30 April 1985)

The self-consistent phonon theories are applied to the calculation of the high-density phase diagram of ^{4}He. We show that inclusion of cubic anharmonic correction terms brings the theoretical phase diagram into agreement with the experimental phase diagram.

I. INTRODUCTION

Recent diamond-anvil-cell measurements on ^{4}He at high pressure[1,2] have produced evidence for a triple point around 300 K with a new solid phase along the melting curve. Subsequent theoretical investigations based on the correlated cell model[3] and extensive molecular dynamics (MD) simulations[4,5] have identified this new phase as a bcc solid. The aim of the present study is to show that a self-consistent harmonic phonon theory, corrected for anharmonic effects, also predicts that the bcc solid is the stable phase of ^{4}He at the temperature of 300 K. Both experimental[6] and theoretical[7,8] studies of the low-density fcc phase of solid helium have revealed that, as the density increases along the melting line, the difference between the experimental phonon dispersion curves and those calculated from the self-consistent harmonic (SCH) theory diminishes. This result indicates that an accurate description of high-density fcc (and presumably also bcc) solid helium near melting could be obtained by adding the cubic anharmonic term to the SCH theory (SCH + C).

In Sec. II we examine phonon theories of various degrees of sophistication in order to establish that the SCH + C approximation is needed to obtain the correct phase diagram of dense solid helium. Using an Einstein approximation for the cubic correction term in the SCH + C theory, we calculate in Sec. III the free energies of the fcc and bcc phases and show that near melting at $T \sim 300$ K the bcc solid is the stable phase.

From a comparison between the phonon dispersion curves obtained from MD simulations and the SCH theory, it appears that the bcc phase is more anharmonic and anisotropic than the fcc phase which explains the shortcoming of the simple approximations considered in Sec. II.

II. THERMODYNAMICS AND PHASE DIAGRAM FROM "SIMPLE" APPROXIMATIONS

Although "simple" approximations, as the harmonic ones, are known to be inadequate to describe the near melting anharmonic solid, they may be of value to study the transition between two solid phases, due to cancellation of errors in both phases. For instance, the free energy difference between two solid structures, say, fcc and bcc, could give information about the relative stability of one phase with respect to the other at a given thermodynamic state. With this in mind we used various approximate theories to calculate the free energy of fcc and bcc solid ^{4}He at $T=400$ K and volume $v=4.51$ cm^3/mole, near the melting line where anharmonic effects are important and the bcc structure known to be stable.[5] The conclusions reached for this point apply also in a density domain near the melting line. The potential used in these calculations was a modified Aziz potential[1] which differs from the original one[9] by a slightly less stiff repulsive part allowing for a better representation of the melting curve.[1,10]

The free-energy results for the fcc and bcc phases obtained from the various "simple" approximations considered in this section are summarized in Table I. First it is seen that the harmonic approximation predicts an unstable bcc phase (due to unstable transverse 110 modes). This instability demonstrates the importance of anharmonic effects in the bcc solid. The high-temperature expansion[11] (including terms up to order β^6, where $\beta=1/k_BT$) of the harmonic free energy is inadequate in the bcc phase insofar as it does not predict this instability. In the fcc phase the high-temperature approximation for the free energy is 5% lower than the exact harmonic result.

The self-consistent phonon theory (SCP) is the most appropriate method of taking account of anharmonic effects in solids. Before discussing the results of the first-order approximation to the SCP theory [the self-consistent harmonic (SCH) theory] and corrections to it, we consider a somewhat simpler approximation, the self-consistent Einstein model (SCE) which consists of minimizing the free energy with respect to the frequency ω_E, of $3N$ independent identical harmonic oscillators (see, e.g., Ref. 12).

For the thermodynamic state considered, the SCE model gives the fcc solid as the stable phase (cf. Table I). The optimum frequency ω_E determined from the SCE model can be used, following Dobson,[13] as a starting point in an iterative solution scheme for the self-consistent har-

TABLE I. Free energy of fcc and bcc solid ^{4}He at $T=400$ K and $v=4.51$ cm^3/mole. All calculations are done with a modified Aziz potential (Ref. 1).

Description	$\frac{\beta F_{\text{fcc}}}{N}$	$\frac{\beta F_{\text{bcc}}}{N}$
Harmonic (momentum expansion)	4.44	4.49
Harmonic (exact)	4.58	unstable (imaginary frequencies for the T110 modes)
Optimum Einstein	5.175	5.319
SCH$_1$-Einstein	4.811	unstable (imaginary frequencies for the T110 modes)
Anisotropic Debye	4.849	4.989
SCH$_1$-Debye	4.810	unstable (imaginary frequencies for the T110 modes)
SCH	4.809	4.825
SCH + CE	4.462	4.395

monic phonon spectrum. If one iteration is performed the corresponding free energy (denoted SCH$_1$-Einstein in Table I) is seen to be in very good agreement with the exact SCH result for the fcc phase, whereas the bcc phase turns out to be unstable. The latter result reinforces our previous conclusion concerning the stronger anharmonicity and indicates anisotropy of the bcc phase. It suggests to resort to a two-frequency optimum Debye spectrum in order to calculate the free energy. The latter is obtained by minimizing the free energy with respect to a longitudinal (ω_{DL}) and a transverse (ω_{DT}) frequency.

The corresponding free-energy values are clearly an improvement on the SCE values despite the fact that the fcc phase is the stable phase for the thermodynamic state considered (cf. Table I, results denoted anisotropic Debye). As for the SCE model, the frequencies ω_{DT} and ω_{DL} obtained for the "anisotropic Debye" model can be used as initial values in Dobson's procedure for determining the phonon frequencies. Performing one iteration (result marked SCH$_1$-Debye in Table I) we find that the bcc phase is unstable.

When extended to a large density and temperature domain the SCE and anisotropic Debye models allow for a qualitative description of the phase diagram of high density solid ^{4}He. The triple point associated with the bcc-fcc transition is predicted at very high temperature, ~ 1000 K (a precise location is not possible because the melting curve is not sufficiently well known[1]), and the domain of the fcc phase in the density-temperature diagram curves back to the $T=0$ K axis as predicted by Young *et al.*[14] However, this result should be considered with caution since the transition pressure at $T=0$ K is 7 Mbar far beyond the validity of the pair potential description of ^{4}He.

Considering the SCH theory corrected for cubic anharmonic terms as a reference to the simple approximations so far considered, Table I shows that the errors on the free energy are rather small in the fcc phase but considerably amplified in the bcc phase leading for most approximations to an unstable behavior. Finally, none of the approximations considered in this section is capable of giving a quantitative description of the fcc-bcc transition line.

III. SELF-CONSISTENT HARMONIC APPROXIMATION AND IMPROVEMENT

A. Self-consistent harmonic approximation

As mentioned above, the SCH approximation is the lowest order self-consistent phonon theory. Since comprehensive reviews are available (see, e.g., Ref. 15), we will state only the central equations of the theory, following the work of Moleko and Glyde.[12]

The frequency $\omega_{\mathbf{q}\lambda}$ of a phonon having wave vector $\mathbf{q}$ and branch λ is calculated from the usual expression of the harmonic theory:

$$\omega^2_{\mathbf{q}\lambda}=\sum_{\mu,\nu}\varepsilon_\mu(\mathbf{q},\lambda)D_{\mu\nu}(\mathbf{q})\varepsilon_\nu(\mathbf{q},\lambda)\ , \tag{1}$$

where $\varepsilon_\mu(\mathbf{q},\lambda)$ is the polarization vector and $D_{\mu\nu}(\mathbf{q})$ the dynamical matrix expressible in terms of the force constants $\Phi_{\mu\nu}(\mathbf{R}_{0l})$ between atoms 0 and l associated with the lattice sites $\mathbf{R}_0$ and $\mathbf{R}_l$ ($\mathbf{R}_{0l}=\mathbf{R}_l-\mathbf{R}_0$),

$$D_{\mu\nu}(\mathbf{q})=\frac{1}{M}\sum_l(e^{-i\mathbf{q}\cdot\mathbf{R}_{0l}}-1)\Phi_{\mu\nu}(\mathbf{R}_{0l})\ . \tag{2}$$

The force constants $\Phi_{\mu\nu}(\mathbf{R}_{0l})$ are the second derivatives of the potential between atoms 0 and l averaged over the distribution, assumed to be Gaussian, of their relative displacements $\mathbf{u}$ from their lattice positions:

$$\begin{aligned}\Phi_{\mu\nu}(\mathbf{R}_{0l})&=\left\langle\frac{\partial}{\partial r_{0,\mu}}\frac{\partial}{\partial r_{l,\nu}}v(r_{0l})\right\rangle\\&=\frac{1}{[(2\pi)^3\det\overleftrightarrow{\Lambda}]^{1/2}}\\&\quad\times\int d\mathbf{u}\exp(-\tfrac{1}{2}\mathbf{u}\cdot\overleftrightarrow{\Lambda}^{-1}\cdot\mathbf{u})\frac{\partial}{\partial r_{0,\mu}}\frac{\partial}{\partial r_{l,\nu}}v(r_{0l})\ ,\end{aligned} \tag{3}$$

where $\mathbf{r}_0=\mathbf{R}_0+\mathbf{u}_0$, $\mathbf{r}_l=\mathbf{R}_l+\mathbf{u}_l$, $\mathbf{r}_{0l}=\mathbf{r}_l-\mathbf{r}_0$, and $\mathbf{u}=\mathbf{u}_l-\mathbf{u}_0$.

The displacement correlation matrix

$$\Lambda_{\mu\nu}(\mathbf{R}_{0l})=\langle u_\mu u_\nu\rangle \tag{4}$$

is related to the frequencies and polarization vectors through

$$\Lambda_{\mu\nu}(\mathbf{R}_{0l})=\frac{\hbar}{MN}\sum_{\mathbf{q},\lambda}(1-e^{i\mathbf{q}\cdot\mathbf{R}_{0l}})\varepsilon_\mu(\mathbf{q},\lambda)\varepsilon_\nu(\mathbf{q},\lambda)\times\frac{1}{\omega_{\mathbf{q}\lambda}}\coth(\beta\hbar\omega_{\mathbf{q}\lambda}/2)\,. \tag{5}$$

The set of coupled equations (1)—(5), which define the SCH approximation, are solved iteratively. The frequencies $\omega_{\mathbf{q}\lambda}$, which are solutions of these equations, minimize the free energy expression

$$\beta F_{\mathrm{SCH}}=\tfrac{1}{2}\beta\sum_{l(\neq 0)}\langle v(r_{0l})\rangle+\sum_{(\mathbf{q},\lambda)}\ln[2\sinh(\beta\hbar\omega_{\mathbf{q}\lambda}/2)]-\tfrac{1}{4}\beta\sum_{(\mathbf{q},\lambda)}\hbar\omega_{\mathbf{q}\lambda}\coth(\beta\hbar\omega_{\mathbf{q}\lambda}/2)\,. \tag{6}$$

For an interaction potential v having spherical symmetry the second derivative of the potential is ($\mathbf{r}\equiv\mathbf{r}_{0l}$)

$$\frac{\partial}{\partial r_\mu}\frac{\partial}{\partial r_\nu}v(r)=(\beta-\alpha)\frac{r_\mu r_\nu}{r^2}+\alpha\delta_{\mu\nu}\,, \tag{7}$$

with $\alpha=(1/r)(\partial v/\partial r)$ and $\beta=\partial^2 v/\partial r^2$.

Following Jayanthi *et al.*[16] we then write the average force constants in the approximate form ($\mathbf{R}=\mathbf{R}_{0l}$)

$$\Phi_{\mu\nu}(\mathbf{R})=\left\langle(\beta-\alpha)\frac{r_\mu r_\nu}{r^2}\right\rangle+\langle\alpha\rangle\delta_{\mu\nu}\simeq\langle(\beta-\alpha)\rangle\left\langle\frac{r_\mu r_\nu}{r^2}\right\rangle+\langle\alpha\rangle\delta_{\mu\nu}\,. \tag{8}$$

The authors of Ref. 16 have shown that for a first-nearest-neighbor interaction, the factorization (8) is actually exact to second order in the displacements $\mathbf{u}$ for an fcc crystal. This result is easily extended to the case of a bcc crystal. To second order in $\mathbf{u}$,

$$\left\langle\frac{r_\mu r_\nu}{r^2}\right\rangle=\frac{R_\mu R_\nu}{R^2}\left[1-\frac{\langle u^2\rangle}{R^2}+4\frac{\langle\mathbf{R}\cdot\mathbf{u}\rangle}{R^4}\right]+\frac{\langle u_\mu u_\nu\rangle}{R^2}-2\frac{\langle(\mathbf{R}\cdot\mathbf{u})(R_\mu u_\nu+R_\nu u_\mu)\rangle}{R^4}\,. \tag{9}$$

Using these expressions we have calculated the frequencies $\omega_{\mathbf{q}\lambda}$ iteratively until a free energy was obtained converged to within two parts in 10^4 (this is achieved with 8 iterations for the fcc solid and 12 for the bcc solid). The sums were carried out over $\frac{1}{48}$ of the total Brillouin zone with a grid equivalent to 3999 points in the full zone for fcc and 3455 points for bcc.

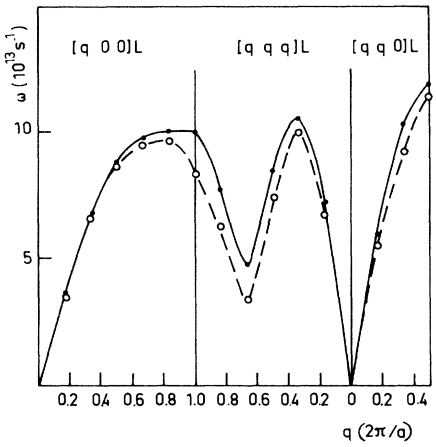

FIG. 2. Same as in Fig. 1 for bcc ^{4}He at $v=4.173$ cm^3/mole.

The phase diagram calculated within the SCH approximation has a triple point at ~ 700 K well above the experimental value (~ 300 K). For the thermodynamic state considered in Table I the stable phase will thus be the fcc phase. This failure can be attributed to the neglect, in the SCH approximation, of the higher-order anharmonic terms arising in the expansion of the crystal potential energy. These terms introduce width and shift in the phonon response function. In Figs. 1 and 2 comparison is made between the dispersion curves for longitudinal phonons calculated from the SCH theory and by MD simulations[5] at 330 K near melting. (The SCH results reported in Figs. 1 and 2 are for the original Aziz potential[9] which has also been used in the MD simulations.[5]) The difference between the SCH and MD dispersion curves appears to be smaller than the difference observed, at lower pressure, between the SCH and experimental dispersion curves for fcc ^{4}He. As in the latter case, the experimental results could be reproduced with good accuracy by a theory (SCH + C) which corrects the SCH approximation for cubic anharmonic terms in the crystal energy expansion;[7,8,17]

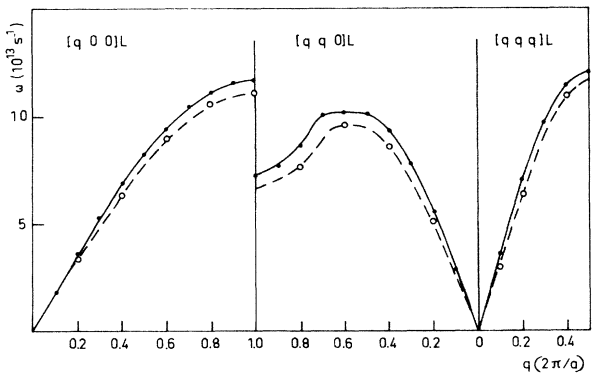

FIG. 1. Dispersion curves for fcc ^{4}He at $T=330$ K and $v=4.165$ cm^3/mole using the Aziz potential (Ref. 9). Solid line, SCH approximation; circles and dotted line, MD simulations.

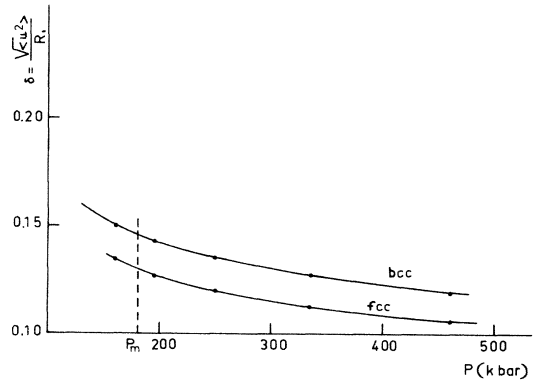

FIG. 3. Lindemann ratio $\delta=(\langle u^2\rangle)^{1/2}/R_1$ versus pressure at $T=400$ K.

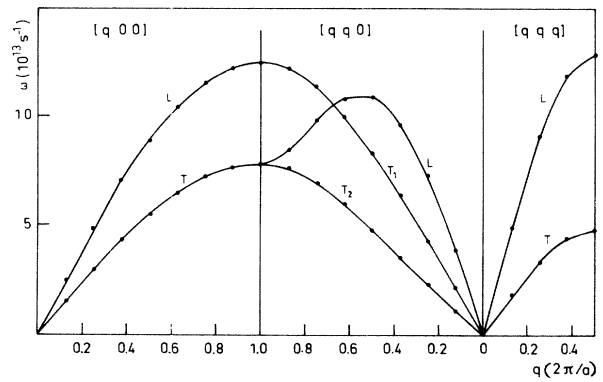

FIG. 4. Dispersion curves for fcc ^{4}He at $T=330$ K and $v=4.21$ cm^3/mole in the SCH approximation. The potential used is the modified Aziz potential of Ref. 1.

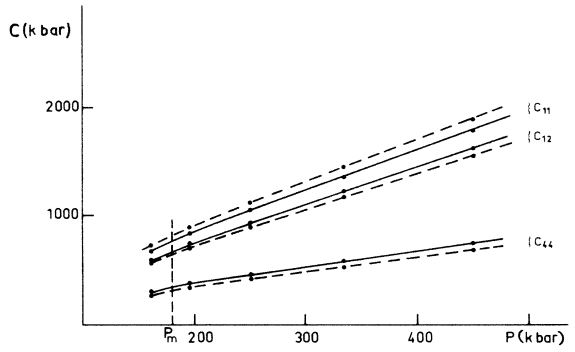

FIG. 6. Isothermal elastic constants at $T=400$ K calculated from the SCH dispersion curves. Solid line, bcc; dotted line, fcc.

such a theory is expected to give good results also in the present case.

From Figs. 1 and 2 we also note that anharmonic effects are somewhat stronger in the bcc than in the fcc phase. This observation is confirmed by the fact that the mean-square displacement of the atoms from their lattice positions is larger in the bcc phase (cf. Fig. 3).

B. Improved self-consistent phonon theory

From Sec. III A it is apparent that accurate values for the free energy could be obtained by including anharmonic cubic terms. A method which treats the cubic anharmonic term as a perturbation correction to $F_{\rm SCH}$ has been introduced by Goldman *et al.*[18] The correction term ΔF_3 to the $F_{\rm SCH}$ free energy is, however, rather complicated, involving a lengthy calculation with a double summation over the Brillouin zone. An estimate can be obtained within the framework of an Einstein approximation.[12,19] This approximation introduces two major simplifications in the calculation of ΔF_3. First, all frequencies $\omega_{\mathbf{q}\lambda}$ are replaced by the same value ω_E obtained as the average of the SCH frequencies

$$\omega_E^2=\frac{1}{3N}\sum_{(\mathbf{q},\lambda)}\omega_{\mathbf{q}\lambda}^2 . \tag{10}$$

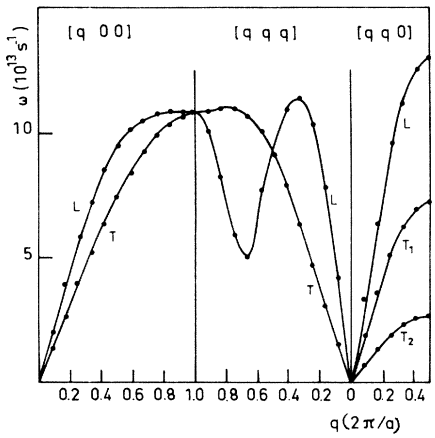

FIG. 5. Same as in Fig. 4 for bcc ^{4}He.

Second, as a consequence, the distribution of displacements $\mathbf{u}$ is spherically symmetric. The final expression reads

$$\Delta F_3^E=-A\frac{\hbar^2}{48M^3\omega_E^4}[12n(\omega_E)^2+12n(\omega_E)+1]$$
$$\times\sum_l\sum_{\alpha,\beta,\gamma}\Phi_{\alpha\beta\gamma}^2(\mathbf{R}_{0l}) , \tag{11}$$

where $\Phi_{\alpha\beta\lambda}$ is the average of the third derivative of the interaction potential over the Gaussian distribution of displacements defined in (3), and

$$n(\omega_E)=(e^{\beta\hbar\omega_E}-1)^{-1} . \tag{12}$$

The constant A is introduced in order to compensate for the fact that by replacing all $\omega_{\mathbf{q}\lambda}$ by the average value ω_E, ΔF_3 will be underestimated ($\Delta F_3\sim\omega^{-4}$). Moleko and Glyde[12] propose the value $A=2.36$ for the case of the fcc solid. When an identical value of A is used for the bcc solid the phase diagram calculated from the free energy,

$$\frac{\beta F_{\rm SCH+CE}}{N}=\frac{\beta F_{\rm SCH}}{N}+\frac{\beta}{N}\Delta F_3^E , \tag{13}$$

is very similar to the one obtained within the SCH approximation, with a slightly lower triple point at 580 K still overly high compared to the experimental value.

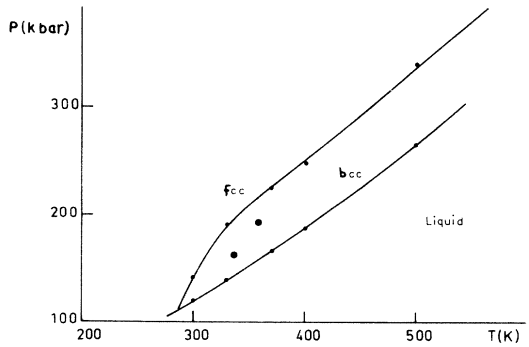

FIG. 7. High-pressure phase diagram of ^{4}He calculated within the SCH + CE approximation. The solid circles denote MD results.

TABLE II. Equilibrium pressure and volumes of the fcc-bcc phase transition in the SCH + CE model; $P_{melting}$ is calculated from a Simon equation (Ref. 22).

T (K)	P (kbar)	v_{fcc} (cm^3/mole)	v_{bcc} (cm^3/mole)	$P_{melting}$
300	141	4.61	4.64	120
330	190	4.24	4.27	140
370	226	4.04	4.07	167
400	249	3.99	4.01	188
500	341	3.61	3.63	266

The authors of Ref. 19 pointed out that the effects of thermal defects should be incorporated into a description of the near melting solid. This is, however, not the case for the present work where the vacancy concentration is expected to be negligible ($\sim 10^{-6}$). The origin of the discrepancy is more likely to lie in the rather crude estimate of ΔF_3. In particular, the constant A need not be the same in the fcc and in the bcc phase, especially since anharmonic effects are larger in the latter phase.

From the MD simulations[5] at $T=330$ K the equilibrium between the two solid phases was obtained for the volumes $v_f=4.165$ cm^3/mole (fcc phase) and $v_b=4.173$ cm^3/mole (bcc phase). For the volume $v=4.169$ cm^3/mole $[=\frac{1}{2}(v_b+v_f)]$ the free energies of both phases would be almost equal: we use this remark to determine the value of the parameter A entering the correction term ΔF_3^E [Eq. (11)] in the bcc phase.

Using the value $A=2.36$ in the fcc phase[12] we find $A=2.77$ in the bcc phase a slightly higher value as expected on the basis of the larger anharmonicity of the bcc phase. Using this value of A the bcc phase is the stable phase for the thermodynamic state $v=4.51$ cm^3/mole and $T=400$ K, as can be seen from Table I.

IV. RESULTS AND CONCLUSION

The dispersion curves calculated in the SCH approximation at $T=330$ K and $v=4.21$ cm^3/mole for the fcc and the bcc structures are shown in Figs. 4 and 5, respectively. The good agreement with the MD results in the long-wavelength region (cf. Figs. 1 and 2) implies that a good estimate of the isothermal elastic constants c_{11}, c_{12}, c_{44} can be obtained.[8,20,21] These are plotted in Fig. 6 as a function of pressure for $T=400$ K. The almost linear dependence on pressure, except in the near melting region, indicates that anharmonic effects are less important than in the low-density solid.[6] The larger value of the ratio $A_N=2c_{44}/(c_{11}-c_{12})$ for the bcc structure stresses again the larger anisotropy of this structure.

At the melting pressure the Lindemann ratio δ (mean-square displacement divided by the nearest-neighbor distance) is equal to 0.15 as expected on the basis of the Lindemann criterion for the thermal melting of a classical solid,[15] indicating a rather classical behavior of very dense helium at $T=\sim 300$ K.

The high-pressure phase diagram of ^{4}He computed from the SCH + CE free energies is shown in Fig. 7 (the values used for A in the expression of ΔF_3^E are those quoted in Sec. III). The domain of the bcc solid along the melting line ends at a triple point with temperature $T=285$ K, close to the experimental value (300 K). Figure 7 also includes two points of the bcc-fcc transition line determined by MD simulations.[5] The discrepancy between the MD and SCH + CE results reflects partly the difference between the potentials used in the MD (original Aziz[9]) and SCH + CE (modified Aziz[1]) calculations, and partly the shortcoming of the SCH + CE approximation.

The volumes of the fcc and bcc phases along the transition line are summarized in Table II. The error on the variation of volume through the transition is estimated to be 50% as a result of interpolation of the free energy curves as a function of volume in the double-tangent Maxwell construction.

To summarize briefly, we have shown that if cubic anharmonic terms in the potential energy are incorporated into the self-consistent phonon theory, the corresponding higher-pressure phase diagram of ^{4}He is in good agreement with the MD results and experiment. Nevertheless, this theory should be viewed only as a "minimal theory" because of the approximate evaluation of the cubic anharmonic term and the neglect of higher-order anharmonic terms in the free-energy expansion.

ACKNOWLEDGMENTS

We wish to acknowledge the continuous interest of J. M. Besson in this work. Laboratoire de Physique des Milieux très Condensés and Laboratoire de Physique Théorique et Hautes Energies are Laboratoires associés au Centre National de la Recherche Scientifique (France).

[1] P. Loubeyre, J. M. Besson, J. P. Pinceaux, and J. P. Hansen, Phys. Rev. Lett. **49**, 1173 (1982).

[2] J. M. Besson, R. Le Toullec, P. Loubeyre, J. P. Pinceaux, and J. P. Hansen, *IX AIRAPT International High Pressure Conference Proceedings,* Vol. 22 of *High Pressure in Science and Technology* (North-Holland, Amsterdam, 1983), Chap. II, p. 13.

[3] P. Loubeyre and J. P. Hansen, Phys. Rev. B **31**, 634 (1985).

[4] D. Levesque, J. J. Weis, and M. L. Klein, Phys. Rev. Lett. **51**, 670 (1983).

[5] D. Levesque, J. J. Weis, and P. Loubeyre (unpublished).

[6] J. Eckert, W. Thomlinson, and G. Shirane, Phys. Rev. B **16**, 1057 (1977); **18**, 3074 (1978).

[7] V. V. Goldman, G. K. Horton, and M. L. Klein, Phys. Rev.

Lett. **24**, 1424 (1970).
[8]H. R. Glyde and V. V. Goldman, J. Low Temp. Phys. **25**, 601 (1976).
[9]R. A. Aziz, V. P. S. Nain, J. S. Carley, W. L. Taylor, and G. T. McConville, J. Chem. Phys. **70**, 4330 (1979).
[10]W. J. Nellis, N. C. Holmes, A. C. Mitchell, R. J. Trainor, G. K. Governo, M. Ross, and D. A. Young, Phys. Rev. Lett. **53**, 1248 (1984).
[11]E. W. Montroll, J. Chem. Phys. **11**, 481 (1943).
[12]L. K. Moleko and H. R. Glyde, Phys. Rev. B **27**, 6019 (1983).
[13]J. F. Dobson, Phys. Lett. **62A**, 368 (1977).
[14]D. A. Young, A. K. McMahan, and M. Ross, Phys. Rev. B **24**, 5119 (1981).
[15]N. R. Werthamer, in *Rare Gas Solids,* edited by M. L. Klein and J. A. Venables (Academic, New York, 1976), p. 265; M. L. Klein and T. R. Koehler, *ibid.*, p. 301.
[16]C. S. Jayanthi, E. Tosatti, and A. Fasolino, Phys. Rev. B **31**, 470 (1985).
[17]W. M. Collins and H. R. Glyde, Phys. Rev. B **18**, 1132 (1978).
[18]V. V. Goldman, G. K. Horton, and M. L. Klein, Phys. Rev. Lett. **21**, 1527 (1968).
[19]L. K. Moleko and H. R. Glyde, Phys. Rev. B **30**, 4215 (1984).
[20]R. A. Cowley, Proc. Phys. Soc. London **90**, 1127 (1967).
[21]V. V. Goldman, G. K. Horton, and M. L. Klein, Phys. Rev. B **4**, 567 (1971).
[22]R. L. Mills, D. H. Liebenberg, and J. C. Bronson, Phys. Rev. B **21**, 5137 (1980).